Microstructures in Cenomanian glauconite from the Isle of Wight, England

HERMAN H. ZUMPE

Department of Geology, Chelsea College (University of London), London, S.W. 3

SUMMARY. Cenomanian glauconite grains from the Isle of Wight often possess a thin, pale green shell or 'corona' of glauconite. Optical investigation led to recognition of two types of microstructure in these shells; an outer layer with tangentially orientated c-axes, and an inner isotropic layer. A third type of layer with radially orientated c-axes occurs both subjacent to the corona and at lower levels in glauconite grains. This latter occurrence is frequently a relic of a former corona, and indicates two or more periods of glauconite formation. The disposition of the microstructures allows some conclusions to be drawn with respect to the depositional history of individual glauconite grains.

GLAUCONITE possessing pale-coloured rims or superficial shells was first observed by Murray and Renard (1891), who described and illustrated such grains from Recent marine sediments. In 1897 Cayeux described similar rims, which he had found on glauconite grains from the Upper Cretaceous of northern France. He noted that the glauconite forming the 'rim' was a superficial differentiation of normal homogeneous or granular glauconite, and he called it 'radiating glauconite'; this was never found on its own. Cayeux showed that the shell covers the whole or part of the surface of glauconite pellets, faithfully following its contours. He also noted its very uniform thickness, about 10 μm, the cleavage perpendicular to the surface of the grain, the distinctive pleochroism, and the characteristically high birefringence. Cayeux termed this shell of pale glauconite the 'corona'. More recently, Carozzi (1958, 1960) has mentioned this surface differentiation of glauconite pellets, and attributed it to recrystallization in the solid phase. Carozzi first described the internal microstructures of glauconite pellets, and he writes that '. . . an internal texture showing irregular concentric rings . . . is the first indication of autochthonous glauconite' (Carozzi, 1958, p. 137). Although Carozzi gives no further details, he was probably referring to the structures described in this paper as internal c-radial layers (figs. 1, 2).

Description of structures

The corona is the pale, yellowish-green shell of glauconite that covers some glauconite pellets. Its thickness only varies within the range 5-15 μm, and averages about 10 μm. On any one grain the thickness is nearly constant. The corona can occasionally be seen to line part of the sides of deep, V-shaped syneresis cracks, and hence must have been formed after the cracks had started to appear. Usually, however, syneresis cracks are later than the corona (fig. 3). The corona consists of two concentric layers that differ profoundly in their optical properties (fig. 1).

The outer layer consists of crystalline glauconite, and is usually continuous around the grain periphery. Under high magnification the faint radially orientated cleavage planes described by Cayeux (1897) can occasionally be recognized. These stop abruptly along the contact with the underlying isotropic layer. Even under low magnifications the outer layer of the corona is quite conspicuous because its pleochroism (α = pale yellowish-green, $\beta = \gamma$ = deeper yellowish-green) and birefringence (medium to high
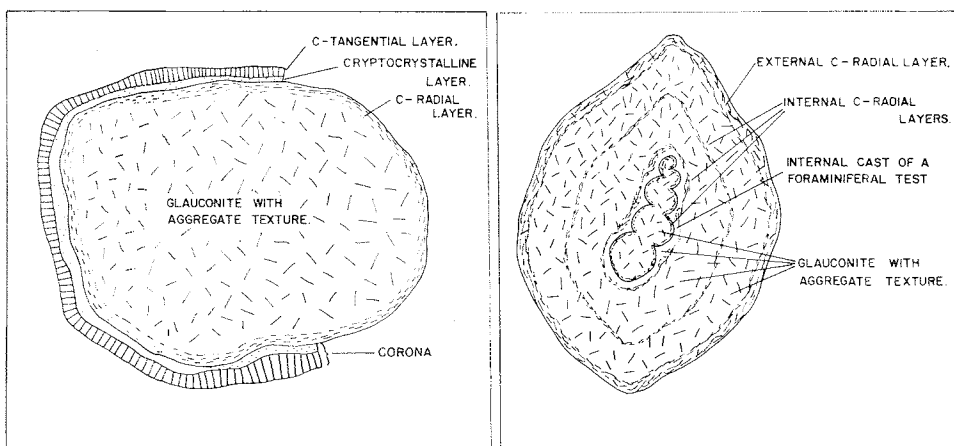

FIGS. 1 and 2: Fig. 1 (left). Cross-section of a glauconite grain showing the two layers of the corona. Over part of the grain the corona has been removed to show the *c*-radial layer immediately underneath it, and also the aggregate texture of the nucleus of the grain. Fig. 2 (right). Cross-section of a glauconite grain having an *external* *c*-radial layer and three *internal* *c*-radial layers. All are separated by thicker shells of aggregate glauconite. The innermost *c*-radial layer represents an internal foraminiferal cast.

first-order colours) are both markedly higher than those of the aggregate glauconite. Optical examination of this layer shows that the radial direction is invariably optically slow (positive); and when this direction is parallel to the vibration plane of the polarizer pleochroic absorption is at a maximum. These features distinguish the outer layer from the other layers, and together with the radial cleavage indicate that in this layer the crystals are regularly oriented with the *c*-axis tangential to the grain periphery. It is proposed that this outer layer be called the *c-tangential layer*.

The inner layer of the corona is not invariably present, and it frequently occurs only in isolated patches underneath the *c*-tangential layer; the intervening boundary is usually irregular. This probably indicates that true equilibrium between the two solid phases has not yet been established, and suggests an arrested recrystallization process. The inner layer is optically almost isotropic, with only a few pin-points of light observable with crossed polars. It also possesses distinctly lower refractive indexes than the rest of the grain. These properties indicate that the inner layer consists of cryptocrystalline or metacolloidal glauconite; and I would propose that it be termed the 'cryptocrystalline layer'.

Structures subjacent to the corona. At the base of the inner layer of the corona there is a third type of layer also showing a preferential orientation, which gradually merges into the randomly orientated glauconite of the main or inner portions of the grain. The boundary with the cryptocrystalline layer, however, is quite sharp. Like the *c*-tangential layer of the corona, the third layer consists of crystalline glauconite, but the *c*-axes of the crystals are approximately radial. Hence the term '*c*-radial layer' is proposed for this structure. It is easily distinguished from the nucleus of the glauconite pellet by its slightly higher polarization colours, which reach up to the middle of the first order of the interference colour scale, compared with the pin-point birefringence of aggregate glauconite.
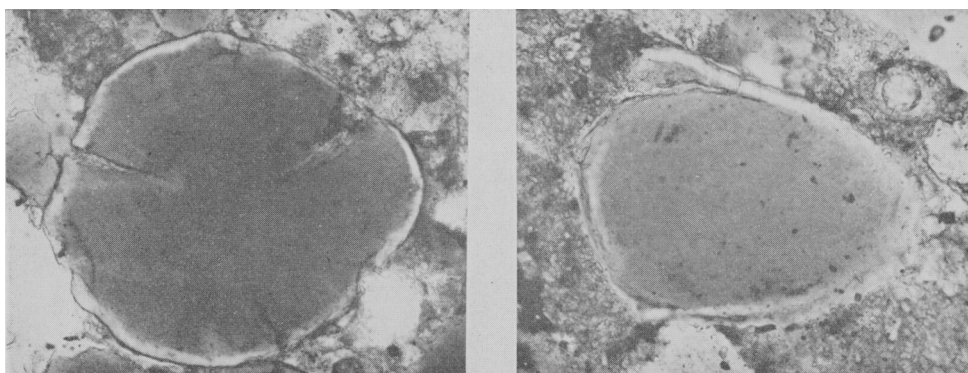

FIGS. 3 and 4: Fig. 3 (left). Photomicrograph of a rounded glauconite grain with a corona. Note the syneresis cracks that formed *after* the corona had been precipitated. Top of Lower Glauconitic Marl, Rocken End. Plane polarized light; × 179. Fig. 4 (right). Photomicrograph of an ellipsoidal glauconite grain with a partially detached corona. Lower Glauconitic Marl, Chale–Niton Road (in cutting of the A3055 about 1 mile south-east of Chale). Plane polarized light; × 229.

The *c*-radial layer thus consists of small flakes of glauconite arranged parallel to the boundary with the adjacent cryptocrystalline layer. This contrast in orientation probably explains why the corona can easily become detached from the remainder of the glauconite pellet as shown in fig. 4. The *c*-radial layer itself, however, is resistant to abrasion because of the interleaving of its glauconite flakes. It is therefore very often preserved in grains from which the corona has been completely removed, and it probably survives several periods of reworking of the sediment.

The *c*-radial layer is always present if there is a corona round a glauconite grain. It also occurs in the glauconite infillings of foraminiferal chambers or sponge spicules, where it lies next to the wall of chamber or spicule. These infillings of glauconite *never* have coronas. It may sometimes form the surface of a glauconite pellet, when its superficial position is probably due to the mechanical removal of the corona or of a foraminiferal test or sponge spicule (fig. 2). Several *c*-radial layers may occur in a single glauconite grain, more or less concentrically arranged about the innermost of these layers. The latter not uncommonly exhibits the outline of the foraminiferal test within which it originated (figs. 2, 5, 6).

Carozzi (1958) was probably referring to these internal c-radial layers when he described 'concentric rings' inside grains of glauconite as evidence of autochthonous grains. If that is so, his conclusion may not be quite correct because internal c-radial layers must indicate several episodes of sediment reworking, each succeeded by glauconite accretion. During this lengthy period of formation the probability of at
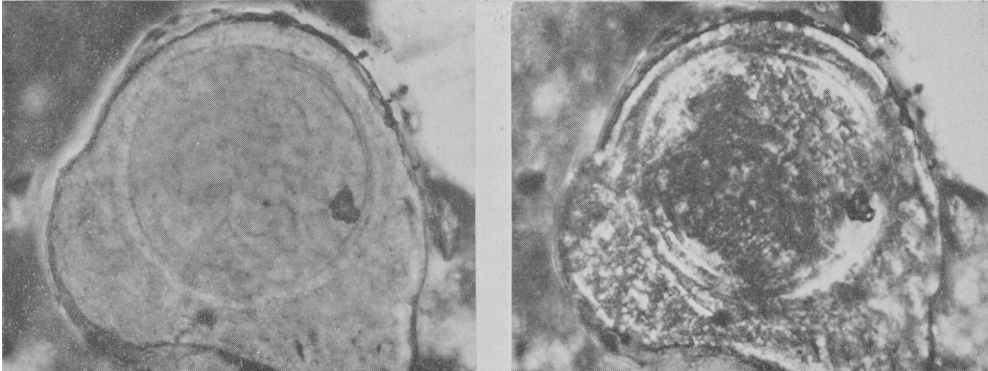
FIGS. 5 and 6: Fig. 5 (left). Photomicrograph of two internal c-radial layers depicting the original spherical glauconite pellet. A period of formation of aggregate glauconite followed, succeeded in turn by the development of a corona consisting entirely of the c-tangential layer. Lower part of the Glauconitic Marl, Chale–Niton Road. Plane polarized light; ×452. Fig. 6 (right). As fig. 5, but with crossed polars and sensitive tint plate; ×452.

least some transport must have been high. On the other hand, abrasion has not been so severe as to remove all internal c-radial layers. Thus glauconite pellets with several internal c-radial layers are unlikely to have been transported very long distances.

Electron microprobe analyses

Two glauconite grains with well-developed coronas were examined with an electron microprobe to obtain a picture of the distribution of certain elements between the aggregate glauconite nucleus and the corona. Photographs were taken of the distribution of potassium, calcium, and total iron. Because of equipment limitations, it was not possible to examine the distributions of sodium, magnesium, or aluminium, nor was it possible to obtain quantitative data for K, Ca, and total Fe (with one exception). For the same reason, a scan for Si could only be obtained for one of the grains.

The corona of the first grain to be examined consisted mainly of a thick crypto-crystalline layer, with negligible thicknesses of sporadically distributed c-tangential and c-radial layers. The results obtained are thus indicative of the compositions of the aggregate glauconite and the cryptocrystalline layer (fig. 7).

The aggregate glauconite of the grain interior shows the expected high concentrations of potassium and iron and a moderate concentration of silicon relative to the marl matrix, which includes a few quartz grains. The concentration of calcium in the aggregate glauconite is very low (bottom left).

The concentrations of these elements in the cryptocrystalline layer are somewhat different. Since silicon proved to be at the detection limit of the microprobe, the results are not particularly reliable. As far as can be seen from the photograph (top left), the background concentration of Si in the matrix is quite high, and that in the cryptocrystalline layer is not noticeably different from it. The potassium concentration (top right) is decidedly lower in the crypto- crystalline layer than in the aggregate glauconite, but still above that in the matrix. The calcium distribution (bottom left) in this corona proved rather sur- prising. Visually, the calcium concentra- tions of the cryptocrystalline layer and the marl matrix appear to be similar. However, these are on the shoulder regions of the sensitiometric curves, and have thus registered as equally low photo- graphic densities. Rapid comparison counts for the amounts of Ca in the matrix and the corona gave a value of $16 \pm 3 \cdot 7 \%$ Ca^{2+} in the cryptocrystalline layer compared with $20 \pm 4 \cdot 6 \%$ Ca^{2+} in the marl matrix. (The amount of Ca^{2+} in

FIG. 7. Electron-microprobe scans of the first grain analysed. Light colour indicates high con- centration. Top left, Si; top right, K; bottom left, Ca; bottom right, Fe. Magnification × 100.

the marl was estimated from insoluble residue percentages, and the limits are the confidence interval of the mean for a 95 % confidence level.) Borchert and Braun (1963) in their analyses of 78 different glauconites found a maximum content of $3 \cdot 5 \%$ CaO, equivalent to about 3 % Ca^{2+}. This must represent about the upper limit of calcium that can be accommodated in the glauconite structure. A value of c. 16 % Ca in the cryptocrystalline layer must mean that at least some 13 % Ca is present as a gross impurity or adsorbed. Microchemical tests have shown that the corona does not react with cold $2N$ hydrochloric acid, and hence does not contain any calcium carbonate; also, the refractive indexes and the birefringence are all too low for a carbonate mineral. Values for the cation adsorption of glauconite appear to be scarce in the literature and vary a lot with particle size; values quoted for glauconite and illitic clays ranged from 25 to 50 meq./100 g. The mean of five values was $35 \pm 12 \cdot 9$ meq./100 g, equivalent to about $0 \cdot 7 \%$ Ca^{2+}; so it seems that only $0 \cdot 5$–1 % of Ca can be adsorbed by colloidal glauconite. Whilst revising this manuscript I noted that in a recent paper Bailey and Atherton (1969) reported finding the carbonate fluorapatite francolite in certain types of glauconite pellets from the Hibernian Greensands (Cretaceous) of Northern Ireland. An analysed glauconite sample contained about 73 % of francolite. It might therefore be possible to explain the high Ca^{2+} content in the corona of this particular glauconite grain by an admixture of c. $31 \pm 8 \cdot 9 \%$ francolite, which would account for the remaining 13 % Ca that cannot be accommodated in the glauconite structure.

The iron concentration (fig. 7, bottom right) in the cryptocrystalline layer was
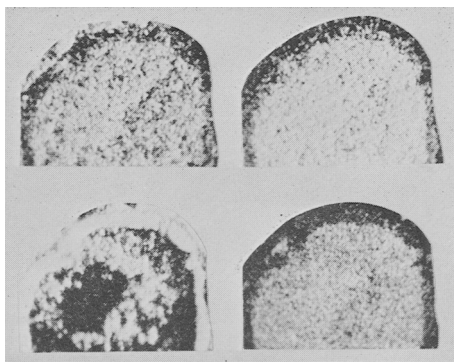
estimated at about 3 % Fe. A few patches of c-tangential layer are optically distin-
guishable in the corona of this grain, and these are just discernible as higher concen-
trations of iron, potassium, and perhaps silicon in the element distribution
photographs.

The estimated concentrations of Si, K, Ca, and total Fe in atomic percentages are:

Element	Matrix	Aggregate glauconite	Cryptocrystalline layer
Si	c. 6 %*	c. 25–45 %	c. 6 %*
K	—	c. 2–3 %	—
Ca	20±5 %	not more than 0·2 %	16±4 %
Fe	—	16–18 %†	c. 3 %

* Near limit of counter sensitivity.
† 16–18 % Fe indicates a 'normal' type of glauconite in the nucleus (Borchert and Braun, 1963).

The second glauconite grain to be examined had well-developed c-tangential and
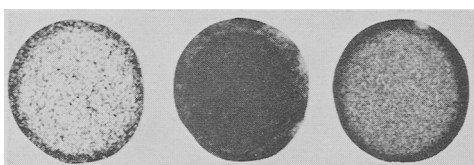c-radial layers. The cryptocrystalline layer was rather thin, but still well developed.

FIG. 8. Electron-microprobe scans of the second
grain analysed. Left, K; middle, Ca; right, Fe.
Magnification ×100.

In the aggregate glauconite there is a
moderate concentration of potassium
(fig. 8, left) as compared with the back-
ground; and it is estimated at about
1–2 % K^+ by rapid comparison counts,
equivalent to about $\frac{1}{4}$–$\frac{1}{2}$ K^+ ion per
formula unit, suggesting a mixed-layer
glauconite (Burst, 1958). The concentra-
tion of Ca (fig. 8, middle) in the
aggregate glauconite is very low. The
concentration of total iron (fig. 8, right) in the aggregate glauconite was measured
using a standard of known Fe content; this gave a value of 11·1 % Fe, which would
suggest that the glauconite is of the low-iron type and probably the variety skolite
(Smulikowski, 1936, 1954; Borchert and Braun, 1963).

In the corona of this grain there is a slight decline in the potassium concentration as
compared with the nucleus. The calcium content in both the c-tangential and c-radial
layers is significantly higher than in the aggregate glauconite. A comparison of the
photographic densities of marl background and corona suggests that the corona
contains 2·5±0·6 % Ca^{2+} (based on insoluble residue analyses of the Glauconitic
Marl). Up to 3 % Ca^{2+} has been found in analyses of glauconite (Borchert and
Braun, 1963), hence a value of 2–3 % is quite normal. The concentration of iron
(fig. 8) in the corona is of the same order of magnitude as that of the glauconite
nucleus, but slightly less, about 9 %.

From these analyses, the aggregate glauconite ranges from the normal to the
aluminium-rich variety (skolite); in the corona, the concentrations of potassium, iron,
and probably silicon are lower than those of the aggregate glauconite, whereas the
calcium concentration is much higher.

Origin of the microstructures

Origin of the corona. The corona has only been observed in glauconite grains *not* enclosed in foraminiferal tests or other faunal remains. This suggests that the corona is formed by the addition of glauconite to the surface of a nucleus of aggregate glauconite. Such a hypothesis is supported by the optical and chemical differences between corona and nucleus, and also by the general presence of the amorphous cryptocrystalline layer; this makes a recrystallization of the aggregate glauconite as suggested by Carozzi (1960) most unlikely. Both Smulikowski (1954) and Gorbunova (1950) ascribed the light yellowish-green colour of the corona to a lower Fe^{3+}/Al ratio compared with the aggregate glauconite. The lower total iron concentration of the corona as shown by the electron microprobe results supports this conclusion. There is no colour difference between the *c*-tangential and cryptocrystalline layers. All this suggests that the corona originated as a precipitate of an impure or proto-glauconite around an existing glauconite nucleus. This process is analogous to the formation of superficial ooliths as described by Carozzi (1960). The glauconite precipitate was probably in the colloidal state, as suggested both by Hadding (1932) and by Smulikowski (1954).

A regular concentric banding consisting of alternating paler and darker layers can very occasionally be seen in the corona. The appearance is similar to the banding so commonly found in calcareous ooliths, and is probably caused by several periods of accretion.

Burst (1958) suggested that glauconite pellets were formed when degraded clays took up potassium, magnesium, and iron into the crystal lattice. The process ended with the formation of glauconite with an ordered mica-type structure (see also Hower, 1961). If Burst's theory is accepted, the relatively low iron and potassium contents of the corona shown by the electron microprobe results would furnish additional evidence that here the process of glauconitization has not been completed. It was cut short by burial of the grain below the sedimentary interface. The meta-colloidal crypto-crystalline layer appears to represent the original state of the corona, and the *c*-tangential layer appears to be a part of the corona that has subsequently recrystallized.

Orientation of the c-tangential layer. All the intermediate stages of the crystallization of the cryptocrystalline layer can be seen in thin sections. These stages range from a very thick cryptocrystalline layer with only a few peripheral patches of *c*-tangential layer to a corona consisting almost entirely of the latter. The 'booklet' type of glauconite has been observed with a surrounding corona consisting entirely of the *c*-tangential layer; even small grains of detrital quartz are sometimes found partially enveloped by a thick *c*-tangential layer of glauconite (Zumpe, 1962). In the great majority of cases, the cryptocrystalline layer of the corona still survives, even if only in discontinuous patches; it is therefore probable that recrystallization started at the periphery of the corona and progressed towards the centre. The alternative, namely that the recrystallization began internally or at the inner boundary of the corona appears most

unlikely in view of the optical evidence, especially since the inner boundary of the
c-tangential layer is so irregular. The recrystallization was almost certainly accom-
panied by the loss of adsorbed water. This fact, together with the low iron content
would account for the refractive index of the cryptocrystalline layer being distinctly
lower than that of the remainder of the corona or the rest of the glauconite pellet
(see Toler and Hower, 1959). Unfortunately it was impossible to measure the refractive
index of the cryptocrystalline layer.

Assuming that the limiting factor governing the speed of recrystallization is the
rate of dehydration of the metacolloidal cryptocrystalline layer, and assuming further
that the highest rate of water loss occurs at the periphery of the corona (because
little water could be taken up by the nucleus of the glauconite pellet), it is clear that
as the c-tangential layer continues to grow thicker, it must increasingly impede the
outward diffusion of the expelled water, until finally the recrystallization is almost
totally inhibited. This process would help to explain why in the large majority of
coronas that have been observed at least some vestiges of the cryptocrystalline layer
still remain along the inner boundary of the corona.

The orientation of the c-tangential layer may be explained by the rates of growth
of the new crystals at the periphery of the corona; this will be controlled by the
supply of uncrystallized material and the orientation of the crystals. The most
abundant supply of uncrystallized glauconite lies concentrically beneath the grain
periphery, and the slowest growth in glauconite crystals, which are similar to those
of the micas in this respect (Kamb, 1959), is in the direction parallel to the c-axis.
Together these factors will favour the development of those crystals that are orientated
with their axis of slowest growth, the c-axis, *tangential* to the boundary between
recrystallized and amorphous glauconite. The well-known fibro-radial and spherulitic
habits of minerals are, at least in part, caused by similar mechanisms.

Stress-fields in hollow spheres. The corona and the layer immediately beneath it may,
as a first approximation, be regarded as a hollow sphere subjected to either internal
or external hydrostatic pressures. It can be readily shown from elementary mechanical
considerations that in the case of a sphere under an external hydrostatic pressure,
both the tangential stresses and the radial stress will be compressional, with the
tangential stresses being greater than the radial stress. Hence the radial stress is a
unique stress axis of relative *tension* oriented radially. Conversely, under an internal
hydrostatic pressure, there is a radially oriented unique stress axis of relative
compression.

Origin and orientation of the c-radial layer. As with the c-tangential layer, the charac-
teristic orientation of the crystals in the c-radial layer and the origin of this layer are
closely interrelated. The various situations in which c-radial layers are found have
already been mentioned. In addition, it is noteworthy that c-radially oriented glauco-
nite has been found to be produced at points of localized external pressure, for
example, where a quartz grain has been squeezed into a glauconite pellet during com-
paction of the sediment.

The peculiar orientation of the c-radial layer may possibly be due either to a primary orientation caused by accretion of tabular glauconite crystals, or to a secondary orientation resulting from the recrystallization of glauconite in an external stress field that is oriented with the major stress axis (an axis of compression in this case) perpendicular to the periphery of the glauconite grain. It should perhaps be emphasized that these two causes are by no means mutually exclusive.

At present the balance of the evidence appears to favour the second possibility. According to Kamb (1959), the c-axis or the pseudo-c-axis of phyllosilicates tends to align itself along the axis of greatest compressive stress in a uniaxial stress-field. Glauconite would therefore be expected to crystallize with its c-axis perpendicular to the grain periphery when the axis of greatest compressive stress is perpendicular to the edge of the grain, or when the two axes of tension lie in a plane tangential to the grain periphery. These two equivalent situations may arise when a glauconite pellet is forming in a foraminiferal test or a sponge spicule canal. In these cases Murray and Renard (1891) and Takahashi (1939) claim that in the course of glauconitization the mineral expands in volume. Alternatively, a glauconite grain may shrink in volume only at the surface, thus producing tensions there to reorientate the aggregate glauconite near the surface into a preferential c-radial orientation. The ease with which a local c-radial orientation is produced at points of contact between quartz and glauconite grains suggests that the glauconite crystals are very sensitive to stress fields.
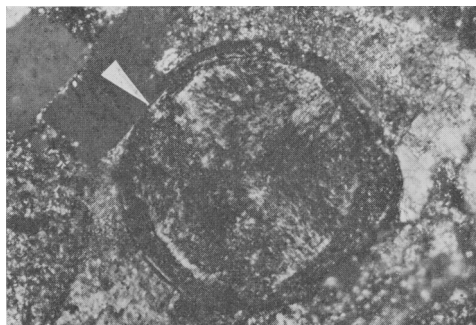

FIG. 9. Photomicrograph ($\times$ 140) showing a lath-shaped quartz grain being pushed into a spherical glauconite grain with a complete corona, changing the c-tangential layer to c-radial as a result of the radially directed pressure at the point of contact. Top of the glauconitic marl, Rocken End. Crossed polars and sensitive tint plate.

REFERENCES

BAILEY (R. J.) and ATHERTON (M. P.), 1969. *Journ. Sedim. Petr.* **39**, 1420–31.
BORCHERT (H.) and BRAUN (H.), 1963. *Chemie der Erde*, **23**, 82–90.
BURST (J. F.), 1958. *Amer. Min.* **43**, 481–97.
CAROZZI (A.), 1958. *Journ. Sedim. Petr.* **28**, 133–50.
—— 1960. *Microscopic Sedimentary Petrography.* New York (Wiley).
CAYEUX (L.), 1897. *Ann. Soc. Geol. Nord*, **4**, 1–589.
[GORBUNOVA (L. I.)] Горбунова (Л. И.), 1950. Акад. наук СССР, Труды Инст. геол. наук (*Acad. Sci. URSS, Trans. Inst. Geol. Sci.*), **114**, Geol. Ser. No. 40, 65–103.
HADDING (A.), 1932. *Medd. Lunds Geol.-Min. Inst., Lunds Univ. Arsskr.* ard. 2, **28**, 1–175 [M.A. 5–378].

HOWER (J.), 1961. *Amer. Min.* **46**, 313–34.

KAMB (W. B.), 1959. *Journ. Geol.* **67**, 153–70.

MURRAY (J.) and RENARD (A. F.), 1891. *Scientific Results, Voyage of H.M.S. Challenger. Report on Deep Sea Deposits.* London.

SMULIKOWSKI (K.), 1936. *Arch. Min. Warszaw,* **14,** 144–80.

—— 1954. Ibid. **18,** 21–120.

TAKAHASHI (J.), 1939. In: TRASK (P. D.) (ed.), 1955. *Recent Marine Sediments. Amer. Ass. Petrol. Geol.*; reprinted by Soc. Econ. Pal. and Min., Spec. Publ. No. 4, 503–12.

TOLER (L. G.) and HOWER (J.), 1959. *Amer. Min.* **44,** 1314–18.

ZUMPE (H. H.), 1962. *The Petrology of the Chloritic Marl (Glauconitic Marl) and the highest Upper Greensand of the Isle of Wight and Swanage Bay.* Unpublished M.Sc. Thesis, University of London.